International Transactions on Electrical Engineering and Computer Science
Naveen et.al., Vol: 2, No: 1, pp: 1-13, March 2023

Energy Management Control for Dual Power Source Powered Electric Vehicle

G. Naveen*, M. Manisha[1]

Abstract: This paper presents a Proposed Energy Management Strategy (PEMS) for an Electric Vehicle (EV) supplied by a fuel cell generator with a storage system based on a super capacitor. A PEMS is needed for hybrid sources to get the energy flow complete numerous sources to feed the power train. Thus, for simulating the studied system under two driving cycles, MATLAB/Simulink has been used. The obtained results proved the good efficiency of the developed PEMS by minimizing the possible fuel consumption of the main power source.

Keywords: Power train, Driving cycles, Energy management, Hydrogen consumption.

1. Introduction

The Fuel Cell (FC) system presents as an attractive choice for vehicular applications, especially when the used FC is a Proton Exchange Membrane (PEM) type [1]. This latter offers a reliable solution for eliminating pollution from conventional sources [2]. To realize maximum efficiency, operate at optimum conditions and increase the reliability of the electric vehicle, the long-term performance of fuel cell systems must be optimized [3]. However, sufficient power generation must be available to the motor system in a way to guarantee the propulsion of the vehicle [4].

Article History
Received: 19- 01-2023; Revised: 05-02-2023;
Accepted: 17-03-2023

*Corresponding author: Department of Electrical and Electronics Engineering, Narasaraopeta Engineering College, Narasaraopeta -522601, Guntur, India.

E-Mail: gubbanaveen231@gmail.com

Ph: +91-9642059091

[1]Department of Electrical and Electronics Engineering, K G Reddy College of Engineering and Technology, Hyderabad-500075, India

E-Mail: manisha.mattapally@gmail.com

To surmount the different problems caused by a lower dynamic output that keeps it from answering early, hybridization between two or more sources is one of the proposed solutions to solve this type of problem [5]. These energy storages extant very effective resolutions for electric vehicles in solving the requirement of FC power generation on different driving operations. This allows the power train to have a more flexible and reliable working presentation [6, 7]. For this reason, studies were oriented toward using hybridization as a solution making use of storage devices along with fuel cells to overcome energy availability problems [8]. The integration of one additional energy source working with a fuel cell guarantees continuous power production for the power train. Energy storage is used especially to minimize the cost of production of hydrogen [9]. This auxiliary source chosen for our work is a super capacitor. It presents a higher dynamic performance than batteries in terms of specific power [10]. The effort offered in this article essentially involves integrating a second source into an electric vehicle system to cover the load demand continuously under two driving phases [11]. For this, An Energy Management technique (EMT) is always needed in a way that ensures maximum stability in the power system while minimizing the fuel cell consumption as low as possible [12].

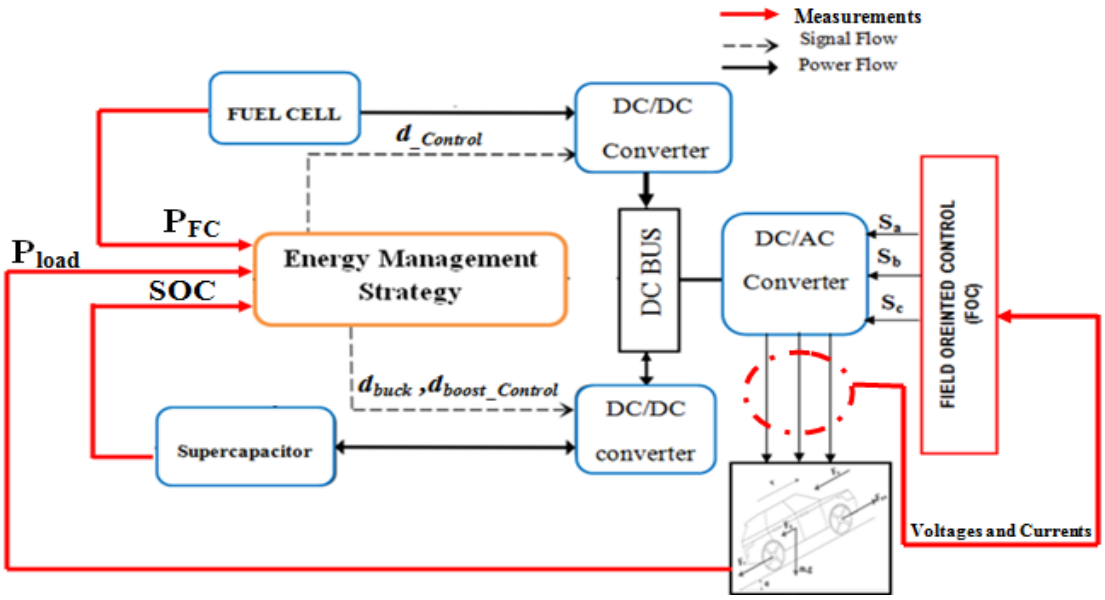

Fig. 1: Adopted Power train configuration

2. General Context of the studied system configuration

The studied energy system is collected of hybrid energy systems supplying a power train as presented in Fig. 1. The studied energy system is consists of

- A two-power source based on: PEM fuel cell generator and a Supercapacitor storage system.
- A Power train propulsion is composed of: DC-AC inverter and a 3 phased asynchronous machine training an electric vehicle
- Two DC-DC converters (Boost and buck/boost) were used to adapt the energy sources to the needs of the connected load.

From another hand, a Proposed Energy Management Technique (PEMT) to controls the flow of energy in this method

- Control the power train and different sources by the use of static converters
- Ensure continuous energy flow optimization to make economic benefits in the power generation of the system.

2.1 PEM Fuel cell

The principle of working of the PEM fuel cell consists of two redox reactions happening at the cathode and the anode [13]. The hydrogen oxidation is realized at the anode side based on (1)

$$2H_2 \rightarrow 4H^+ + 4e^- \quad (1)$$

The oxygen reduction takes place at the cathode side based on (2) [29].

$$O_2 + 4H^+ + 4e^- \rightarrow 2H_2O \quad (2)$$

The resulting overall reaction can be written as in (3).

$$2H_2 + O_2 \longrightarrow 2H_2O + Heat \quad (3)$$

To take into account the physical phenomena occurring at the fuel cell level. (4) give the generated Stack voltage [13]

$$V_{Stack} = (E - U_{con} - U_{act} - U_{ohm})N_{cell} \quad (4)$$

Where:

- N_{cell}: number of cells mounted in series
- V_{FC} : Fuel Cell output Voltage.
- E: Theoretical Potential of the Cell.
- U_{con}: Concentration Voltage Losses.
- U_{act}: Activation Voltage Losses.
- U_{ohm}: Ohmic Voltage Losses.

The EC structure of the buck converter is shown in Fig. 2.

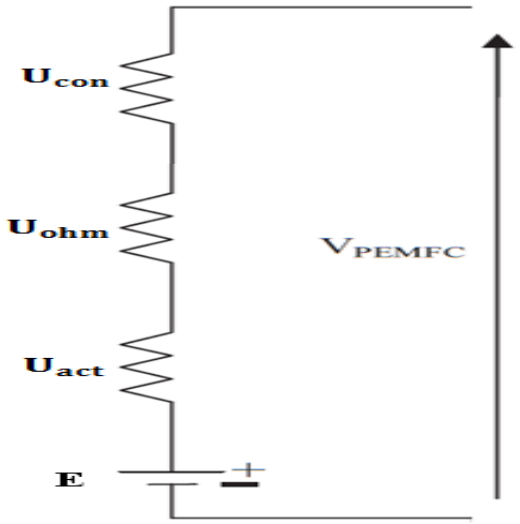

Fig. 2: EC model of Fuel cell

2.2. Supercapacitor

Several circuit models of the super capacitor (sup) are presented in [14, 15]. This energy storage device is the most recommended choice to provide the highest efficiency with a fast load response. The RC model of the sup is shown in Fig.3. The sup is related to a bidirectional Buck-Boost DC-DC converter to raise the voltage in one direction and buck it down in the other according to the operating mode (charging or discharging). Fig. 3 presents the sup electric circuit.

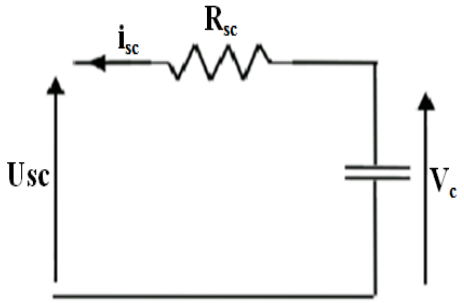

Fig. 3: RC model of the sup

The output voltage of the Sup which is given by (5)

$$U_{sc} = V_c - R_{sc} i_{sc} \quad (5)$$

Where:
R_{sc}: is equivalent series resistance,
V_c: is open single cell's voltage,
i_{sc} is a single cell's current

Table. 1: Parameters of the test system

Components	Parameters	Values
PEM fuel cell	Power	85KW
	Voltage	280V
	Nominal Current	300A
Supercapacitor	Rated capacitance	63F
	Rated Voltage	125V
Vehicle	Vehicle mass	1300 kg
	Air density	1.2Kg/m^3
	Aerodynamic coefficient (A_f)	0.3m^2
specification	Acceleration due to gravity (g)	9.8m/s^2

3. Developed DC/DC converters controllers

3.1. Boost converter Control description

The DC-DC converter must be applied to adapt the low voltage generated by the FC to the required DC bus high-voltage [16]. The electrical schematic boost converter and its control are represented in Fig. 4.

The output voltage (V_{bus}) can be expressed in (6)

$$V_{bus} = d.\, V_{FC} \quad (6)$$

With: d is the duty cycle

Thus, the control scheme developed for the PEM fuel cell essentially consists of a PI controller. This structure is used to reduce the error between the produced current and the reference current to find the duty cycle value recommended to control the PWM generator.

3.2. Control principle of the Buck/Boost converter

Several topologies of bidirectional converters can be divided into two main types as follows: Non-Isolated Converters and Isolated Converters [17]. The bidirectional DC-DC converter is a strong element in interfacing storage devices and DC loads thanks to its ability to ensure power flow in two directions [18]. Figure.5 shows a non-isolated buck/boost converter.

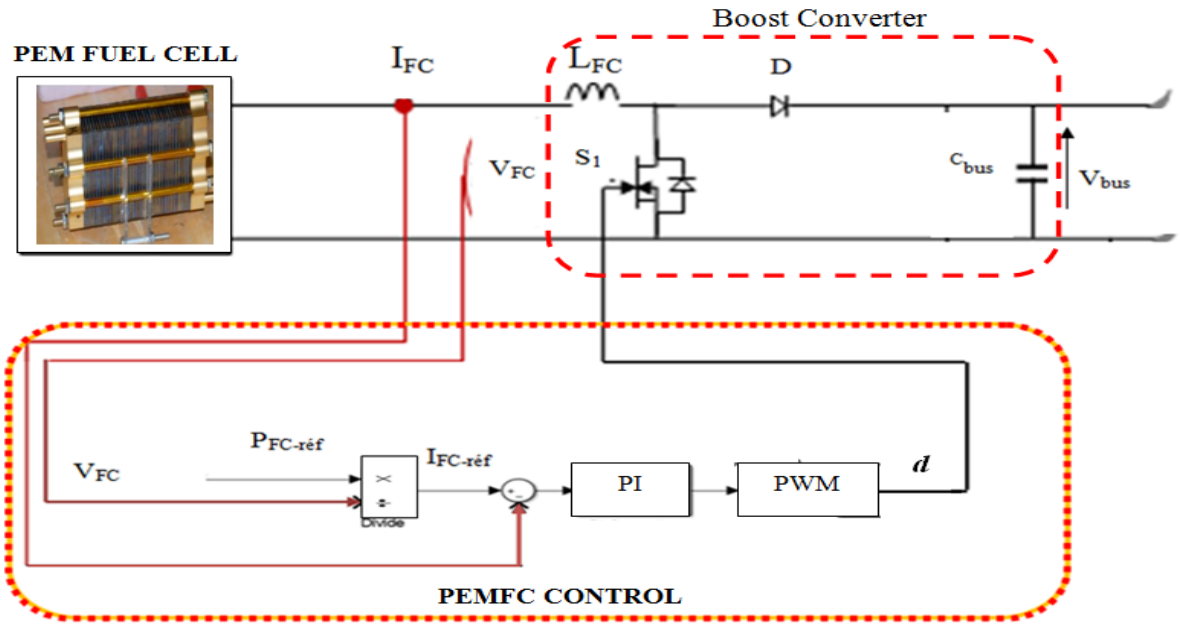

Fig. 4: Control scheme of the FC

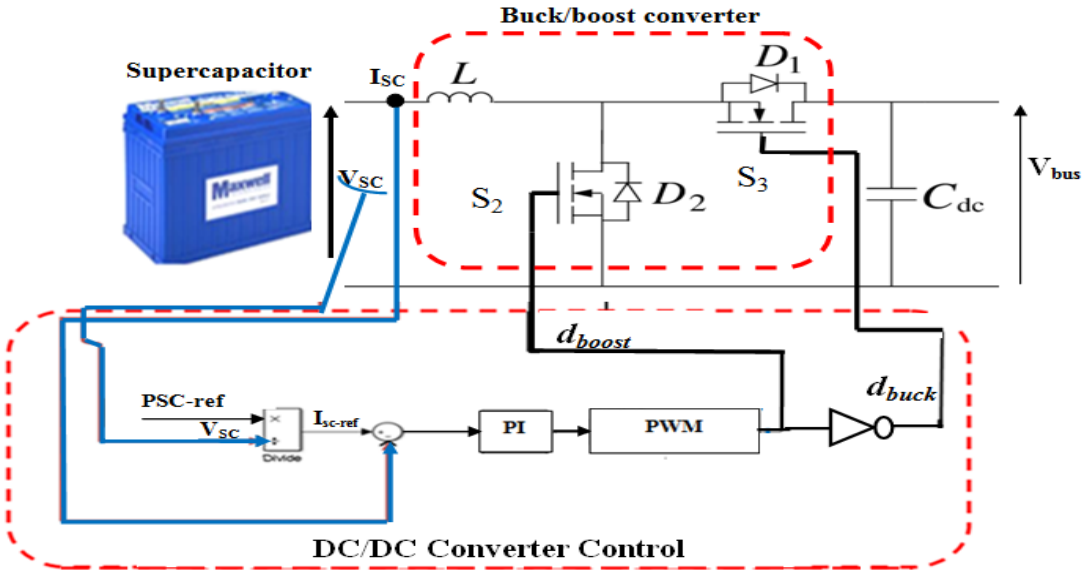

Fig. 5: Super capacitor Control scheme

The operating mode of the converter is determined according to its switches state: S_2 open and S_3 closed: the system operates as a Buck converter. Thus, (7) can express the relation between *Vsc* and *Vbus*

$$V_{sc} = \frac{V_{bus}}{1-d_{buck}} \quad (7)$$

S_2 closed and S_3 open: the structure operates as a Boost converter. Thus, (8) can express the relation between *Vsc* and *Vbus*

$$V_{bus} = d_{boost}.V_{sc} \quad (8)$$

The proposed control structure presented in Fig.5 consists of a buck/boost DC-DC converter managed by a PWM signal generator, which produces control signals of the converter's switch based on the duty cycle value received by applying a PI control action [19]. The different generated control signals by PEMS are

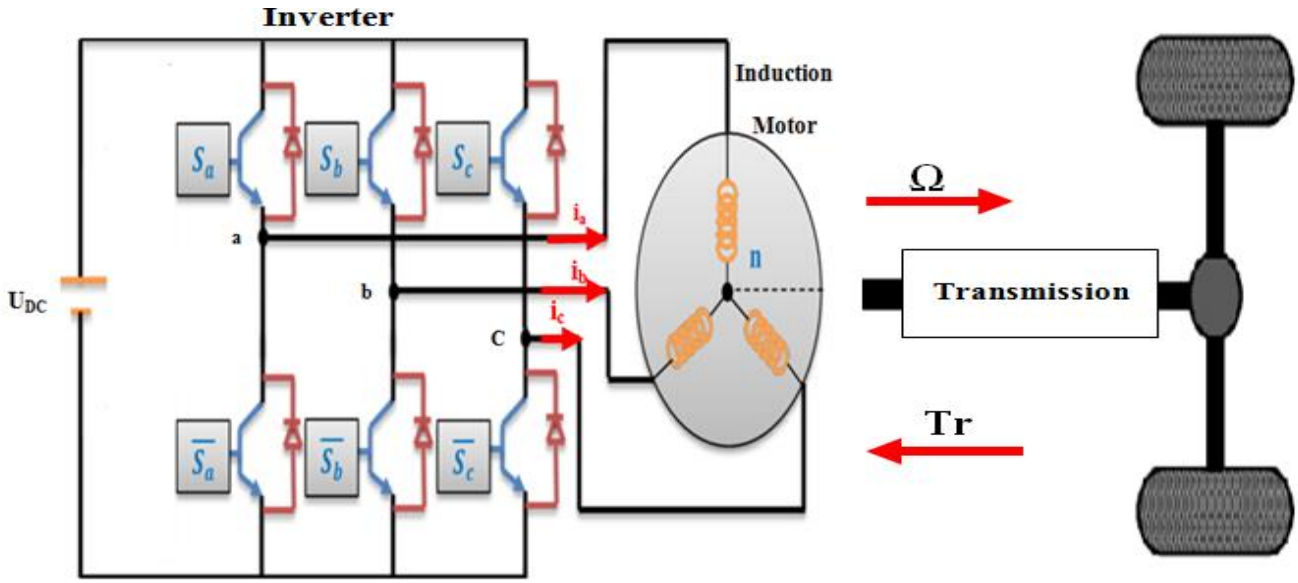

Fig. 6: Descriptive schematic of the power train

$P_{SC\text{-}ref}$: which is the power reference of the SC. It is equal to a positive value for the charging operation and a negative value for the discharging one.

$P_{FC\text{-}ref}$: which is the power reference of the PEM fuel cell.

4. Modeling and Control of the power train

Fig. 6 shows different parts of the power train system which is composed of: a 3-phased voltage inverter and a3 phased asynchronous motor training vehicle [20].

4.1 DC/AC Inverter

The inverter converts the DC power into a 3-phase AC power to adapt the power delivered by the two generators to the power needs of the asynchronous machine [21]. The DC-AC inverter is always needed especially in the speed control of the induction motor. This converter allows obtaining a perfectly three-phase current system from a DC voltage source, thanks to a well-defined opening/closing sequence of its switching cells [22]. The following matrix form given by (9) can express the line-to-neutral voltages:

$$\begin{cases} V_a = \frac{U_{DC}}{3}(2S_a - S_b - S_c) \\ V_b = \frac{U_{DC}}{3}(2S_b - S_a - S_c) \\ V_c = \frac{U_{DC}}{3}(2S_c - S_a - S_b) \end{cases} \quad (9)$$

Where:

- S_i : is the control signal corresponding to the K_i switch (With $i=1,2,3$)
- $S_i=0$ to open the K_i switch and close the K'_i.
- $S_i=1$ to close the K_i switch and open the K'_i.

4.2 Modeling and control description of Asynchronous machine

Based on [23], the model of the AM (a, b,c) frame can be written as given by (10)

$$\begin{aligned} [V_{sabc}] &= [R_s].[I_{sabc}] + \frac{d[\phi_{sabc}]}{dt} \\ [V_{rabc}] &= [R_r].[I_{rabc}] + \frac{d[\phi_{rabc}]}{dt} \\ [\phi_{sabc}] &= [L_{ss}].[I_{sabc}] + [L_{sr}].[I_{rabc}] \\ [\phi_{rabc}] &= [L_{rs}].[I_{rabc}] + [L_{rr}].[I_{rabc}] \end{aligned} \quad (10)$$

The mechanical model of the AM can be articulated as in (11) [23]:

$$T_{em} - T_r - f\Omega = J\frac{d\Omega}{dt} \quad (11)$$

Where:

f : Coefficient of viscous friction.

J : Inertia moment of rotating masses.

T_{em} : Electromagnetic torque.

T_r : Resistive torque.

Ω : Rotor electric speed.

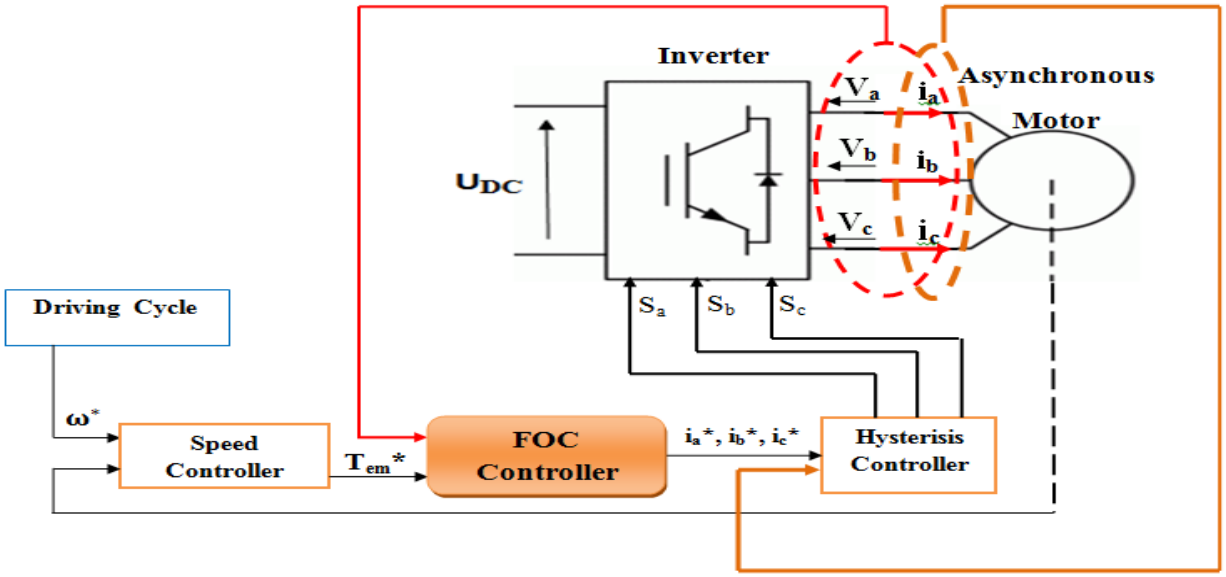

Fig. 7: Adopted speed control scheme

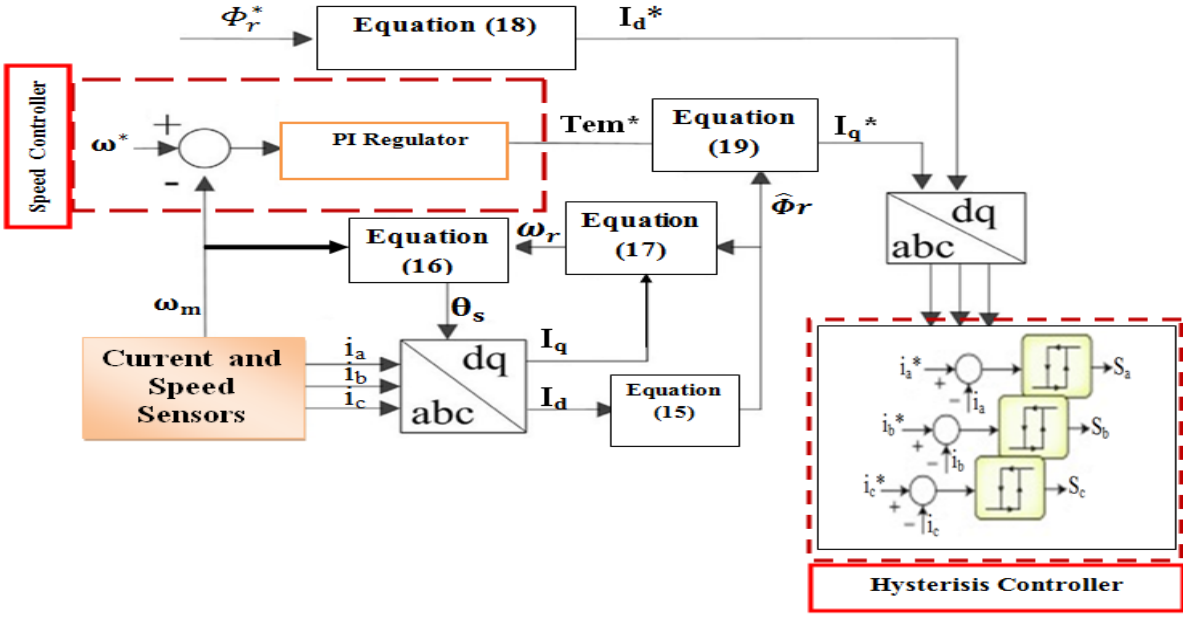

Fig.8: FOC control working principle

V_{sabc} and i_{sabc}: are respectively the voltages and currents at the stator in a,b,c frame ϕ_{sabc} and ϕ_{rabc}: vectors of Stator flux and rotor flux.

The resistive torque (T_r) of the vehicle system (transmission/reducer system +wheels) is proportional to the difference of its resisting forces. (12) Give the resistive torque expression [24].

$$T_r = \frac{R_{wheel}}{r_{red}}\left(F_r + F_a + F_p\right) \quad (12)$$

The resistive forces expression is given by (13)

$$F_r(t) = MgC_r cos\left(\alpha(t)\right)$$

$$F_a(t) = \frac{1}{2}\rho_{air}A_f C_x V_{Veh}^2(t) \quad (13)$$

$$F_p = Mg\sin(\alpha(t))$$

The equations as given by (14) can be arranged in the (d, q) frame.

$$\begin{cases}[V_{sdq}] = [R_s][I_{sdq}] + \frac{d}{dt}[\phi_{sdq}] \\ [V_{rdq}] = [R_r][I_{rdq}] + \frac{d}{dt}[\phi_{rdq}] \end{cases} \quad (14)$$

Different control techniques of speed regulation are studied in the literature [25-26]. The Field Oriented Control (FOC) method is recommended in this research to develop the speed control of asynchronous machine [26]. Fig. 7 shows the detailed control scheme adopted for speed control of the power train via the 3 phased inverters. The detailed FOC structure is described in Fig. 8. This technique control is mainly composed essentially of three blocs:

Block 1: PARK and PARK inverse transformation
Park transformation is recommended to attain the two-phase system of the asynchronous machine on the (d, q) frame correlated to the rotating field from the initial three-phase system on the (a, b, c) frame.
Block 2: Speed controller. A PI controller is the most used one among several others to compute the torque reference (Tem*)
Block 3: Hysteresis Controller. This technique consists in comparing the three phase's current and reference current to generate control signals of the inverter's switches. The equations described the FOC control are given as [26]:

The rotor flux estimate is given by (15).

$$\hat{\Phi}r = \frac{Msrids}{1+p.Tr} \quad (15)$$

With Tr is the rotor time constant.

The angular pulsationθ_s is defined by (16)

$$\theta_s = \int(\omega_s)dt \quad (16)$$

Where:

$$\omega_s = \omega_m + \omega_r = np\Omega_m + \frac{Msr}{Tr}\frac{iqs}{\hat{\Phi}r} \quad (17)$$

ω_r is the rotor electric pulsation.
ω_m is the rotor electric pulsation.

The reference currents I_{ds}^* and I_{qs}^* are defined using (18) and (19).

$$I_d^* = \frac{\Phi_r^*}{M} \quad (18)$$

$$I_q^* = \frac{T_{em}^*}{\frac{3pM}{2L_r}\hat{\Phi}r} \quad (19)$$

4.3 Design Process of the approach developed

The chief objective of this method is to determine the optimal power references for the fuel cell generator ($P_{FC\text{-}ref}$) and storage device ($P_{SC\text{-}ref}$). These power references are used to produce the control signals for the DC/DC converters ensuring an optimized system configuration.Figure.9 presents the Flowchart principle of PEMS.

Thus, the PEM Mainly ensures:

- The reduction of fuel consumption, as well as the guarantee of power continuous accessibility to gratify power train difficulties during the different driving cycles.
- Edge the use of the fuel cell and activity of the storage device as much as possible to ensure the power generation of the system in a way to ensure an economic working performance of the PEMFC by reducing as possible its hydrogen consumption

Where:
Mode 1: is the steady-speed phase
Mode 2: is the braking phase
Mode 3: is the traction phase

5. Simulation results and discussions

In this segment, simulations of less than two driving cycles are supported to test, and prove the efficiency and toughness of the PEMS. The obtained results are given respectively in Figures.10-15 under two driving cycles (Table.2). The SOC of SC for the two driving cycles is respectively given in Fig. 12 and Fig.13. Remarkably, a discharging process has been done when there is the load demand exceeds the available energy from the fuel cell. In this context, the Energy Storage System provides the needed power to guarantee the well-achievement of peak power and minimize fuel consumption. Otherwise, it's remarkable that a charging process has been done by the storage device under the braking phase of the vehicle. Thus, two simulation scenarios (mentioned in Table.3) are carried under two driving cycles to evaluate the hydrogen consumption: (The attained results are specified in Fig. 14 and Fig. 15).

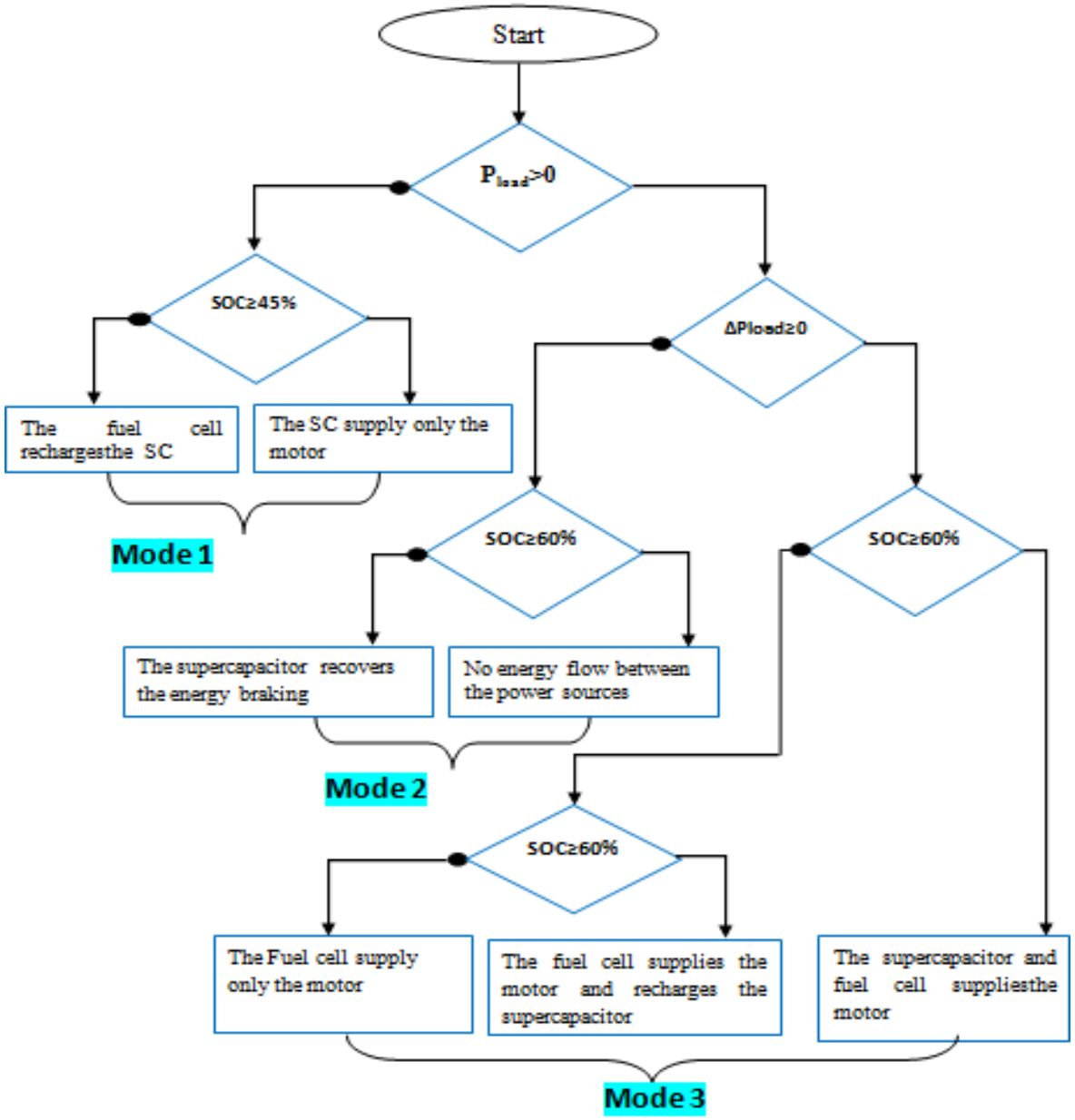

Fig.9: Working principle of the PEMS

The first simulation scenario is made in the total absence of SC. The result is shown in Fig.14. The second simulation scenario is made when the PEMS is implemented. The result is given in Figure.15 by comparing the hydrogen consumption in the two presented scenarios (Fig. 14 and 15), it is clear that the PEMS proves a remarkable minimization in hydrogen is consumption (Table. 3). We note a reduction of 6 g and 18 g respectively for ECE-15 and 10-15 mode driving cycles. As we can see in Tab.3, the PEMS has guaranteed a 46 % and 39% gain in hydrogen consumption respectively for ECE-15 and 10-15 driving cycles. Thus, the obtained results proved good efficiency of the developed PEMS and its main objectives are well ensured. We can conclude that the PEMS is very efficient in deciding on energy sources management and proves its efficiency in controlling the flow of overproduced energy or the lack of energy by controlling the charging and discharging cycles of the storage device. Table.3 sums up the results attained by simulations on the Matlab-Simulink area. The economic benefits of hydrogen consumption of the developed PEMS are well ensured.

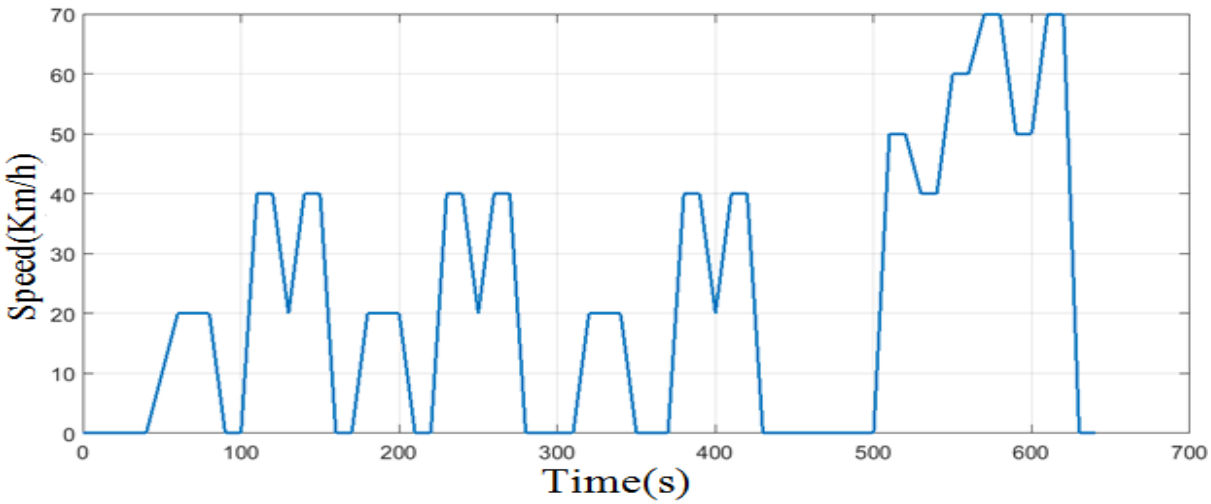

Fig. 10:10-15 mode cycles

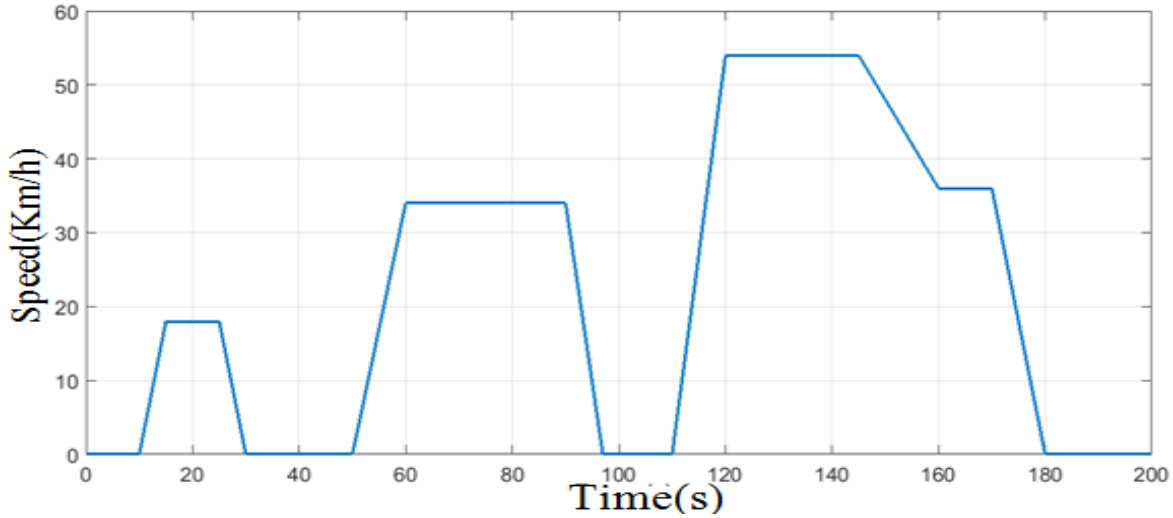

Fig. 11: ECE-15 cycle

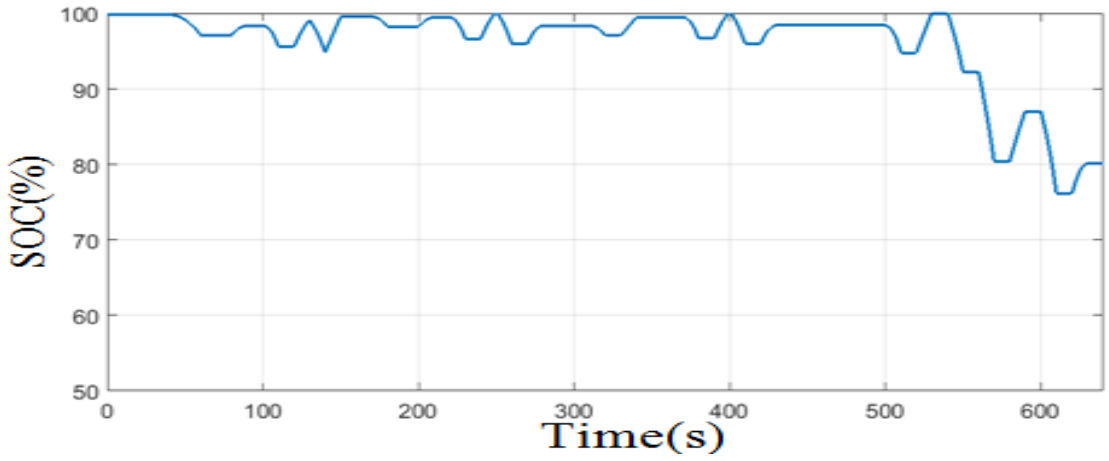

Fig. 12: SOC Variation under 10-15 cycle

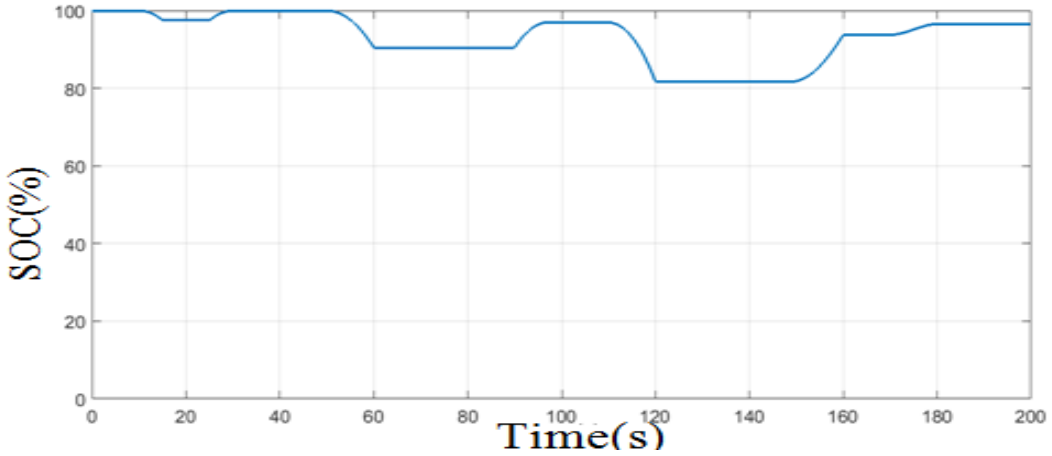

Fig. 13: SOC variation under ECE-15 cycle

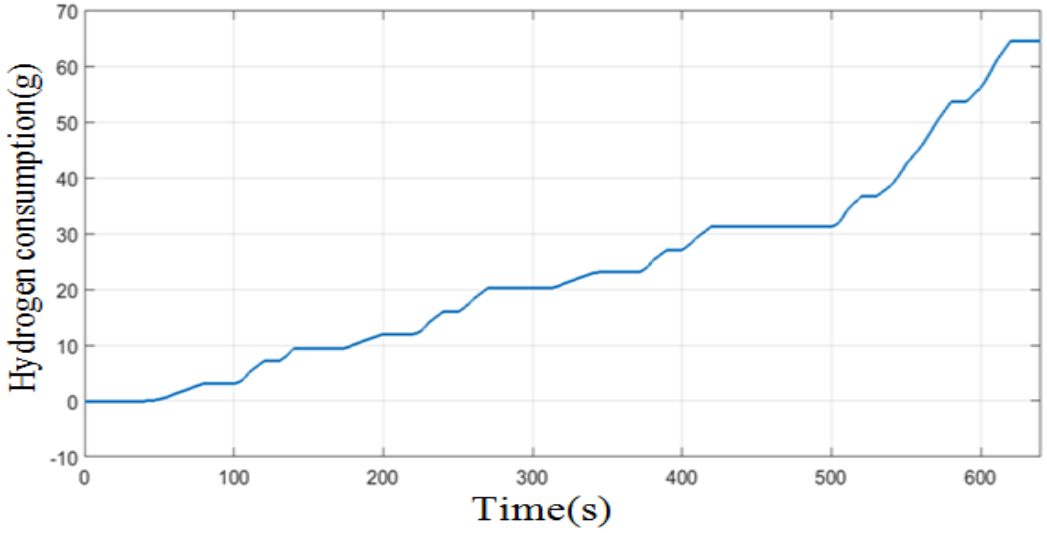

(a)

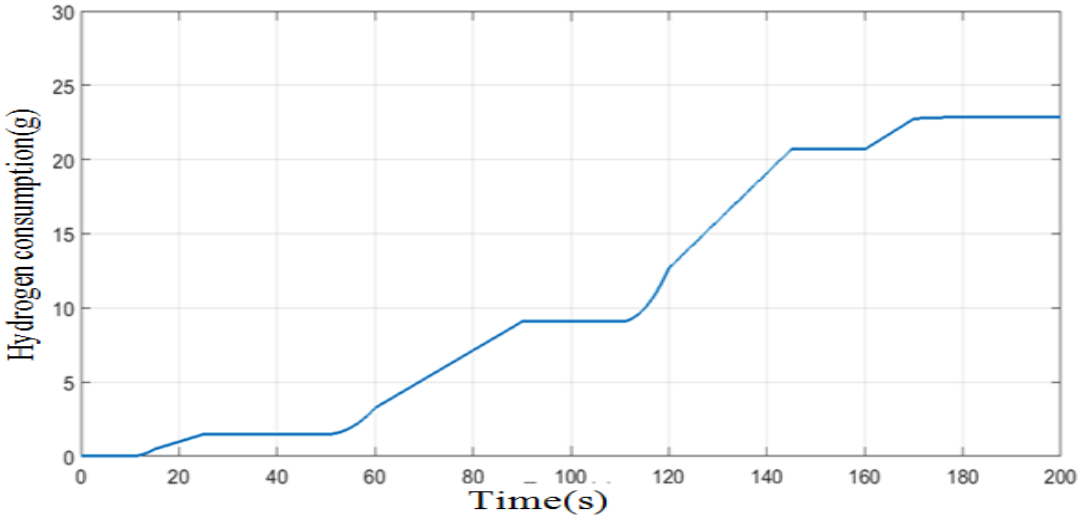

(b)

Fig. 14: Hydrogen Consumption in absence of SC (a) under 10-15 cycles; (b) under ECE-15 cycle

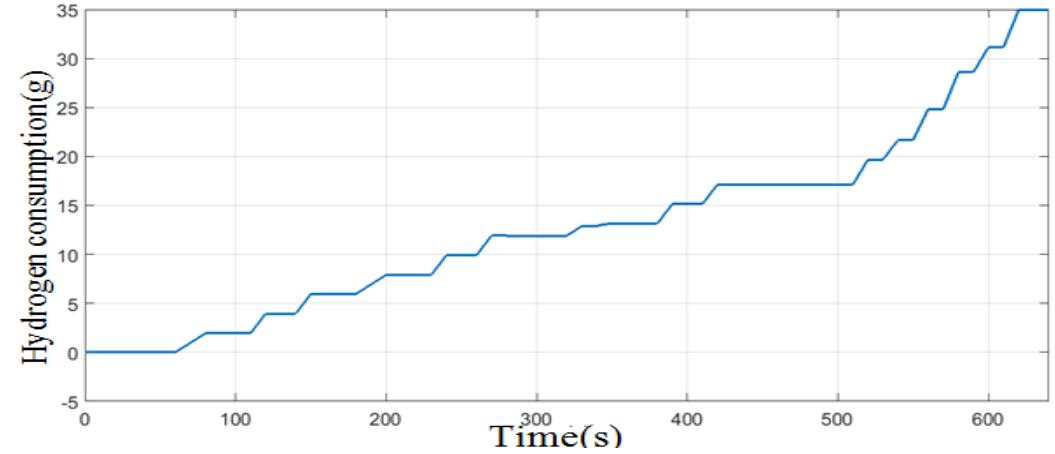

(a)

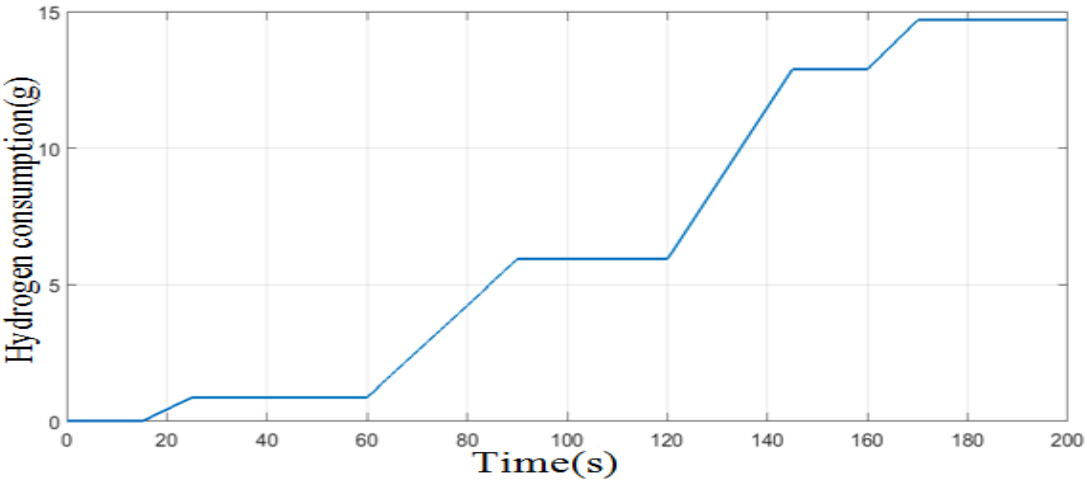

(b)

Fig. 15: Hydrogen Consumption with PEMS (a) under 10-15 cycle; (b) under ECE-15 cycle.

Table. 2: Driving cycles parameters

Cycles ECE-15		10-15 mode
Total time(s)	195	640
Maximum speed(km/h)	57	70

Table. 3: Hydrogen consumption evaluation

Cycles ECE-15		10-15 mode
Hydrogen Consumption without PEMS (g)	65	23
Hydrogen Consumption with PEMS (g)	35	14
Hydrogen gain (%)	46	39

6. Conclusion

Testing simulations realized on Matlab-Simulink proved good efficiency of the developed PEMS and its main objectives are well ensured. The results obtained shows the success of the approach established in a way to achieve the flow of energy among the dissimilar sources to perimeter the use of the fuel cell and exploit the storage system as much as possible during transient's phases of the vehicle

Conflict of Interest

The authors declare that they do not have any conflict of interest

References

[1] W. Andari, S. Ghozzi, H. Allagui and A. Mami, "Design, Modeling and Energy Management of a PEM Fuel Cell / Supercapacitor Hybrid Vehicle", *International Journal of Advanced Computer Science and Applications*, Vol. 8, No. 1, pp. 273-278, 2017.

[2] M. Uzunoglu, O. C. Onar "Modeling, control and simulation of a PV/FC/UC based hybrid power generation system for stand-alone applications", *Renewable Energy*, Vol. 34, No. 5, pp. 509-520, 2009.

[3] W. Andari, S. Ghozzi, H. Allagui, A. Mami "Optimization of Hydrogen Consumption for Fuel Cell Hybrid Vehicle", *Indian journal and sciences*, Vol. 11, No. 2, pp. 1-9, 2018

[4] F. El-Shatter, M. N. Eskandar, M. T. Hagry, "Technical note Hybrid PV/fuel cell system design and simulation", *Renewable Energy*, Vol. 10, No. 5, pp.1-10, 2002.

[5] W. Jiang, B. Fahimi "Active Current Sharing and Source Management in Fuel Cell–Battery Hybrid Power System", *IEEE Transactions on Industrial Electronics*, Vol. 57, No. 2, pp. 752-761, 2010.

[6] M. H. Nehrir, C. Wang, K. Strunz "A Review of Hybrid Renewable/Alternative Energy Systems for Electric Power Generation: Configurations, Control, and Applications", *IEEE Transactions on Sustainable Energy*, Vol. 2, No. 4, pp. 392-403, 2011.

[7] J. Ke, M. Yang, X. Ruan and M. Xu "Three-level bidirectional converter for fuel-cell/battery hybrid power system", *IEEE Transactions on Industrial Electronics*, Vol. 57, No. 6, pp. 1976-1986, 2009.

[8] A. Chauhan, R Saini "A review on Integrated Renewable Energy System based power generation for stand-alone applications: Configurations, storage options, sizing methodologies and control", *Renewable and Sustainable Energy Reviews*, Vol. 38, No. 2, pp. 99-120, 2014.

[9] Y. Atesm, O. Erdinc "Energy management of an FC/UC hybrid vehicular power system using a combined neural network-wavelet transform based strategy", *International Journal of Hydrogen Energy*, Vol. 35, No. 2, pp.774-783, 2010.

[10] T. Yalcinoz, "Improved dynamic performance of hybrid PEM fuel cells and ultra capacitors for portable applications", *International Journal of Hydrogen Energy*, Vol. 20, No. 2, pp. 1932-1940, 2008.

[11] T. Bambang "Energy Management of Fuel Cell/Battery/ Super capacitor Hybrid Power Sources Using Model Predictive Control", *IEEE Transactions on Industrial Informatics*, Vol. 10, No. 4, pp. 1992-2002, 2014.

[12] W. Andari, A. Khadhrawi, S. Ghozzi, H. Allagui, A. Mami "Energy Management Strategy of a Fuel Cell Electric Vehicle: Design and Implementation", *International Journal of Renewable Energy Research*, Vol. 7, No. 3, pp. 1154-1164, 2017.

[13] E. Banguero, A. Correcher "A Review on Battery Charging and DischargingControl Strategies: Application to Renewable Energy Systems", *Energies*, Vol. 11, No. 10, pp. 1021-1030, 2018.

[14] T. Phatiphat, R. Stephane, "Analysis of supercapacitor as second source based on fuel cell power generation", I*EEE Transactions on Energy Conversion*, Vol. 24, No. 1, pp. 247e55, 2009.

[15] B. Jerome, D. Sebastien, "Fuel-cell hybrid powertrain: toward minimization of hydrogen consumption", I*EEE Transactions on Vehicular Technology*, Vol. 58, No. 1, pp. 3168-3176, 2009

[16] S. Chen, T. Liang "A Cascaded High Step-up DC-DC Converter with Single Switch for Micro source Applications", *IEEE Transactions on Power Electronics* Vol. 26, No. 4, pp. 1146-1153, 2011.

[17] D. M. Miracle, "Design and Control of a Modular Multilevel DC/DC Converter for Regenerative Applications", *IEEE Transactions on Power Electronics*, Vol. 28, No. 8, pp. 3970-3979, 2013.

[18] D. Sasi , "A High Step up DC-DC Converter using Cascade Cockcroft Walton Voltage Multiplier", *IOSR Journal of Electrical and Electronics Engineering*,Vol.22, No.5, 2012.

[19] K. Ddine "Design and Modeling of DC/ DC Boost Converter for Mobile Device Applications", *International Journal of Science and Technology*, Vol.2, No. 5, pp. 394-401, 2013.

[20] K. Laaroussi, M. Rouff, "Implementation of a Fuzzy Logic System to Tune a PI Controller Applied to an Induction Motor", *Advances in*

Electrical and Computer Engineering, Vol. 9, No. 3, pp. 107-113, 2009.

[21] B. Venkata, A. Mallikarjuna, "Modelling And Simulation of A Hysteresis Band Pulse Width Modulated Current Controller Applied To A Three Phase Voltage Source Inverter By Using Mat lab", *International Journal of Advanced Research in Electrical, Electronics and Instrumentation Engineering*, Vol. 2, No. 3, pp. 4378-4387, 2013.

[22] B. Vural, A. R. Boynuegri, I. O. Nakir "Fuel cell and ultra-capacitor hybridization: A prototype test bench based analysis of different energy management strategies for vehicular applications", *International Journal Hydrogen Energy*, Vol. 35, No. 20, pp. 11161-11171, 2010.

[23] F. Culić, Dumnić, "Optimal Fuzzy Controller Tuned by TV-PSO for Induction Motor Speed Control", *Advances in Electrical and Computer Engineering*, Vol.11, No. 1, pp. 49-54, 2011.

[24] W. Andari, S. Ghozzi, H. Allagui, A. Mami, "Control Strategy of Fuel Cell/Supercapacitor Hybrid Propulsion System for an Electric Vehicle", *International Journal of Renewable Energy Research*, Vol. 10, No. 1, pp. 464-473, 2020.

[25] M. Jemli, H. B. Azza, "Real-time implementation of IRFOC for Single-Phase Induction Motor", *Simulation Modelling Practice and Theory*, Vol. 17, No. 6, pp. 1071-1080, 2009.

[26] R. D. Lorenzet, D. W. Novotny, "A Control System Perspective of Field Oriented Control for AC Servo Drives", *Proceeding of on Controls Engineering Exposition*, 1988.

***